Generated using the official AMS LaTeX template v6.1

Large climate model ensembles reveal underdispersion in seasonal Atlantic tropical cyclone counts

E. L. Levin[a] G. A. Vecchi,[b,c] G. Villarini,[c,d]

[a] *Program in Atmospheric and Oceanic Sciences, Princeton University*

[b] *Department of Geosciences, Princeton University*

[c] *High Meadows Environmental Institute, Princeton University*

[d] *Department of Civil and Environmental Engineering, Princeton University*

Corresponding author: Emma Levin, emma.levin@princeton.edu

ABSTRACT: Seasonal Atlantic tropical cyclone (TC) counts are commonly modeled as a conditional Poisson process, implying that the distribution of possible seasonal outcomes—the range of TC counts that could plausibly occur in a given year—exhibits equidispersion for a given climate state, with its variance equal to its mean. This assumption underlies many statistical frameworks used for seasonal TC prediction and risk assessment, yet to the best of our knowledge has not been extensively tested directly. Using large ensembles from physics-based climate models (AM2.5-C360 and HiRAM) and a deep learning-based climate emulator (ACE2; Ai2 Climate Emulator version 2), we examine the distributional properties of seasonal TC counts in a controlled modeling framework. Across all models and years, we find that the ensemble distribution of within-season TC counts is systematically underdispersed relative to the Poisson distribution, with ensemble variances smaller than their corresponding means. This result provides evidence against modeling the SST-conditioned Atlantic TC count distribution with a Poisson distribution and instead supports the use of the Binomial distribution. This representation of the Atlantic TC counts implies the following physical interpretation of TC genesis: TCs develop in two stages 1) first from a finite number of seed disturbances, and 2) followed by a seed-TC transition that is governed by large-scale environmental conditions. We fit seasonal TC count distributions from a 1,000-member ACE2 ensemble to the Poisson and Binomial distributions and find statistical evidence that the Binomial formulation provides a better fit to TC count distributions. The Poisson assumption is not supported by current climate model simulations, given that simulated seasonal TC counts are more constrained than implied by traditional Poisson-based frameworks.

SIGNIFICANCE STATEMENT: Seasonal Atlantic tropical cyclone (TC) forecasts are critical for risk preparedness, energy planning, and insurance decision-making. Many statistical models used for these forecasts assume that TCs occur randomly, following a Poisson process. Leveraging unprecedentedly large ensembles from state-of-the-art physics-based and deep-learning climate models, we show that simulated seasonal TC counts systematically violate this assumption. Instead, TC counts are more constrained. This behavior is consistent with a physical picture in which TCs arise from a finite number of precursor disturbances ('seeds') whose likelihood of development depends on the large-scale environment. These results motivate more physically grounded statistical models for seasonal TC prediction.

1. Introduction

North Atlantic Tropical cyclones (TCs) can cause tens to hundreds of billions of dollars in damage annually in the United States, Americas, and Caribbean (Klotzbach et al. 2018), as well as mortality both coincident with the storm and for the years following (Young and Hsiang 2024). Understanding the controls on seasonal TC activity and developing accurate seasonal forecasts are an element of risk preparedness, energy planning, and insurance decision-making. Seasonal outlooks, issued prior to the climatological June through November TC season, predict the number of storms that will form throughout the season. These forecasts are generated using a range of modeling approaches, including dynamical climate models (e.g., Zhao et al. 2010; Chen and Lin 2013; Vecchi et al. 2014; Murakami et al. 2016b, 2025), deep learning (DL)–based weather prediction models (Zhang et al. 2025), and statistical or statistical–dynamical frameworks (e.g., Vecchi et al. 2011; Villarini et al. 2019). Seasonal TC predictions will necessarily be probabilistic in nature (Vecchi et al. 2014), so understanding both the expected TC activity and the plausible deviations from it are essential.

Statistical and statistical–dynamical approaches relate large-scale environmental conditions, such as sea surface temperature (SST), vertical wind shear, and atmospheric humidity, to seasonal Atlantic TC activity. Based on the statistical relationships of large-scale conditions to TCs, these approaches model the plausible distribution of seasonal TC counts conditioned on the large-scale environment for the given year. Early statistical studies (e.g., Gray 1984; Gray et al. 1992) used linear regression to link environmental predictors to TC counts, but such approaches can yield non-integer predictions that are not physically meaningful for discrete storm counts. Subsequent developments innovatively addressed this limitation by explicitly modeling TC counts using discrete probability distributions conditioned on the large-scale environment. The canonical choice has been the Poisson distribution (e.g., Elsner and Jagger 2004, 2006; Jagger and Elsner 2010; Villarini et al. 2012; Davis et al. 2015; Murakami et al. 2016a), which provides a natural framework for count data. Additionally, Villarini et al. (2010) and Li et al. (2023) went to length to explore whether a Poisson model or Negative Binomial discrete model was better to fit the conditional distribution of possible seasonal TC counts, and found that the Poisson model was better suited.

If the conditional seasonal Atlantic TC count distribution follows a Poisson distribution, Atlantic TCs are assumed follow a Poisson process. Under this assumption, there is no upper limit to the number of TC formation trials, there is a small probability that such trials will result in successful TC genesis at any moment during the season, and TCs are assumed to form independent of each other. Therefore, throughout the duration of the season, the accumulation of many possible TC formation trials results in a limited number of storms. This finite seasonal Atlantic TC occurrence rate serves as the sole parameter of the conditional Poisson distribution, which represents the expected level of seasonal TC activity. It is this parameter that statistical and statistical-dynamical studies fit as a function of the large-scale environment using Poisson regression techniques. A key implication of the Poisson assumption is equidispersion, meaning that the variance of the seasonal TC count distribution equals its mean.

The Poisson formulation is attractive due to its mathematical simplicity and minimal parameterization with one free parameter (i.e., seasonal rate parameter), and it is often motivated by viewing TC formation as the outcome of many random independent trials with a low probability of success at any given time (Blitzstein and Hwang 2014). However, the assumption that seasonal TC counts are equidispersed is a modeling convenience and statistical fit from several models (Villarini et al. 2010), rather than a physically derived constraint.

Several alternative discrete distributions have been proposed to represent seasonal TC counts. For example, Villarini et al. (2010) and Li et al. (2023) explored a Negative Binomial conditional distribution, which allows for overdispersion relative to the Poisson model. In contrast, Vecchi et al. (2019) and Hsieh et al. (2020) propose that climatological TC activity be viewed through a Binomial framework in which TC formation is viewed as a sequence of Bernoulli trials, with a finite number of precursor disturbances or seeds providing the number of trials for a given season. In this formulation, both seed frequency and the probability that a seed develops into a TC depend on the large-scale environment, although the climate dependence of each is different. Previous studies have demonstrated the utility of Binomial-type frameworks for describing TC variability across a range of timescales, including the annual cycle (Yang et al. 2021) and longer-term climate variability and idealized experiments (Vecchi et al. 2019; Hsieh et al. 2020, 2022, 2023), especially in the Atlantic basin (Levin et al. 2026b).

These different distributions imply fundamentally different dispersion properties of the conditional seasonal TC count distribution. In this study, we use the term dispersion to refer to the relationship between the variance and mean of the conditional count distribution, rather than the relationship between ensemble spread and forecast error commonly evaluated in ensemble prediction systems. Specifically, dispersion is evaluated relative to the Poisson expectation that the variance equals the mean: equidispersion refers to a variance equal to the mean, overdispersion refers to a variance larger than the mean, and underdispersion refers to a variance smaller than the mean (Johnson et al. 2005). Therefore, while the Poisson distribution is equidispersed, the Negative Binomial distribution yields overdispersed counts, and the Binomial distribution produces underdispersed counts.

The conditional Atlantic TC count dispersion plays a key role in seasonal TC outlooks because it governs the range of possible outcomes. Differences in dispersion between various SST-conditioned Atlantic TC count distributions can change the likelihood of extreme events, which have societal and economic consequences. Despite its importance, the equidispersion assumption underlying the Poisson formulation has rarely been tested directly, largely due to limited sample sizes in observations and traditional modeling frameworks.

A rigorous evaluation of the appropriate conditional distribution for seasonal TC counts requires examining the distribution of simulated or forecasted counts across a large ensemble for a given season. Each ensemble member is prescribed identical SST or large-scale environmental forcing but different atmospheric initial conditions, representing a plausible realization of that season's TC activity. Confidence in quantifying dispersion and performing goodness-of-fit tests for discrete count distributions therefore requires a sufficiently large number of ensemble members, as these higher moments are less well constrained in typical dynamical model ensembles (order ten members).

Traditional seasonal TC prediction systems from physics-based numerical models are generally limited in ensemble size because of substantial computational costs. For example, the seasonal forecasting systems described in Murakami et al. (2025) and Zhang et al. (2025) employ approximately ten to fifteen and 20 ensemble members, respectively, and the AM2.5-C360 and HiRAM simulations used to examine multidecadal variability in Kortum et al. (2024) and Levin et al. (2026b) are limited to five to ten ensemble members. Such ensemble sizes are insufficient to robustly assess the distributional form and dispersion properties of seasonal TC counts.

Recent advances in DL–based weather and climate models provide an opportunity to overcome this limitation. Once trained, these models can be run efficiently at a fraction of the computational cost required by conventional dynamical models, enabling the generation of very large ensembles (e.g., Bi et al. 2023; Chen et al. 2023; Lam et al. 2023; Lang et al. 2024; Kochkov et al. 2024; Watt-Meyer et al. 2025). These systems have been shown to realistically reproduce TC characteristics across subseasonal to interannual timescales (Chien et al. 2025) and recover a well-calibrated representation of internal variability of seasonal TC activity (Levin et al. 2026a).

In this study, we leverage large ensembles generated from SST-forced atmosphere-only models to directly sample the conditional distribution of seasonal TC activity given a prescribed large-scale climate state. Specifically, we analyze idealized and historical simulations from two atmosphere-only models developed at the Geophysical Fluid Dynamics Laboratory (GFDL), AM2.5-C360 and HiRAM, as well as a state-of-the-art DL-based climate emulator, ACE2. Ensemble members are generated under identical SST boundary forcing but with different atmospheric initial conditions, such that each member represents a distinct, physically plausible realization of TC activity conditioned on the same SST-forced environment. This large-ensemble approach enables the distribution of possible seasonal TC outcomes to be estimated directly from the ensemble spread rather than requiring an apriori assumption about the form for the conditional distribution, as is necessary in statistical-dynamical frameworks. In particular, we leverage a 1,000-member ACE2 ensemble to robustly characterize the SST-conditioned distribution of seasonal Atlantic TC counts and evaluate its statistical properties, including dispersion.

This study addresses the following research question: Do seasonal Atlantic TC counts produced by state-of-the-art climate models satisfy the equidispersion implied by a Poisson process, or do they exhibit systematic departures consistent with alternative generative mechanisms? We further examine whether these properties are consistent across models with fundamentally different internal dynamics. In the following sections, we describe the models and experiments used in this analysis (Section 2), present evidence that seasonal Atlantic TC counts are underdispersed relative to Poisson expectations (Section 3), and discuss the implications of these findings for statistical TC prediction models, physical interpretations of TC genesis, and the use of large ensembles from AI-based climate emulators (Section 4).

2. Methods and data

a. Models and experiments

To simulate large ensembles of annual Atlantic TC seasons, we use a combination of global high-resolution dynamical atmospheric models and an DL-based climate and weather emulator. The dynamical models used in this study were developed at GFDL and implemented on the Princeton computing system (Zhao et al. 2009; Chen and Lin 2013; Hsieh et al. 2020; Chan et al. 2021; Yang et al. 2021; Kortum et al. 2024; Levin et al. 2026b): AM2.5-C360 and HiRAM. Both models have been shown to realistically simulate TC and hurricane climatology (Zhao et al. 2009, 2010; Yang et al. 2021), including TC tracks (Kortum et al. 2024), as well as interannual-to-multidecadal Atlantic TC variability (Chan et al. 2021; Levin et al. 2026b).

AM2.5-C360 and HiRAM share the same finite-volume cubed-sphere dynamical core but differ in their horizontal resolution and atmospheric physics, particularly their representation of moist convection. HiRAM has a horizontal resolution of approximately 50 km and uses the shallow convection parameterization of Bretherton et al. (2004). In contrast, AM2.5-C360 has a higher horizontal resolution of approximately 25 km and uses the relaxed Arakawa–Schubert convection parameterization scheme (Moorthi and Suarez 1992). The AM2.5-C360 configuration is similar to the high-resolution atmospheric component of the coupled GFDL HiFLOR model (Murakami et al. 2015), which has been shown to realistically simulate and predict Category 4–5 hurricanes. Consistent with this capability, AM2.5-C360 has also been shown to capture interannual variability in Atlantic major hurricane frequency (Levin et al. 2026a).

We analyze a suite of idealized experiments with the dynamical models forced with distinct SST patterns. To generate large ensembles of TC activity under identical boundary forcing, each experiment is integrated for several decades, typically between 30 and 200 years. Each simulated year represents a plausible realization of TC activity under the prescribed SST pattern, since the monthly SST boundary conditions remain fixed and the only source of variability arises from differences in initial conditions. In this way, each experiment produces 30 to 200 ensemble members of seasonal TC activity. The experiments, summarized in Table 1, largely follow the designs used in previous studies (e.g., Hsieh et al. 2020, 2022).

Each experiment is based on a control simulation in which both models are forced with a repeating annual cycle of climatological SSTs averaged over the 1986–2005 baseline period, consistent with the reference period used in the CMIP5 climate change experimental framework. This climatological cycle is repeated for 200 years in HiRAM and 100 years in AM2.5-C360 after a 10-year spin-up. The resulting long-term means represent the statistically steady-state climatological baselines for each model. TCs are tracked for every simulated year, and because the boundary conditions do not vary, each year is treated as an independent ensemble member characterizing TC activity under mean 1986–2005 conditions. Because the autocorrelation in aggregate of annual TC statistics is effectively zero, differences in ensemble members represent the result of internal atmospheric variability. Additional experiments apply perturbations to this baseline, including a uniform $+2K$ and $+4K$ SST warming and $-2K$ and $-4K$ SST cooling to the 1986-2005 climatology. We also analyze several experiments to represent isolated perturbations of greenhouse gas radiative forcing, where we double ($2\times CO_2$) carbon dioxide concentrations and multiply carbon dioxide concentrations by five ($p5\times CO2$) relative to the control experiment. Additionally, we explore an experiment where we both double atmospheric carbon dioxide concentrations and uniformly warm the climatological 1986-2005 SSTs by $+2K$ ($+2K\ 2\times CO_2$). These experiments are also described in Hsieh et al. (2020); Yang et al. (2021); Hsieh et al. (2022); Kortum et al. (2024); Eusebi et al. (2025); Levin et al. (2026b).

To investigate the influence of El Niño Southern Oscillation on Atlantic TC activity, we also explore El Niño and La Niña experiments, which are explained in Hsieh et al. (2022). In these cases, the prescribed SST annual cycles are derived from the strongest events between 1980 and 2015. The El Niño experiment (+Niño) uses the mean SST fields from nine years with Oceanic

TABLE 1. List of idealized experiments used in this study, which are also used in Hsieh et al. (2020); Yang et al. (2021); Hsieh et al. (2022); Kortum et al. (2024); Eusebi et al. (2025); Levin et al. (2026b).

Experiment	Years (and models)	Description
CTL	100 (AM2.5-C360), 200 (HiRAM)	1986-2005 monthly climatological mean SSTs
+2K	50 (both)	Uniform SST warming
+4K	50 (HiRAM only)	Uniform SST warming
-2K	30 (HiRAM only)	Uniform SST cooling
-4K	30 (HiRAM only)	Uniform SST cooling
2×CO_2	50 (both)	CO_2 doubling
p5×CO_2	40 (HiRAM only)	×5 CO_2 increase
+2K & 2×CO_2	50 (both)	Uniform SST warming and CO_2 doubling
+Niño	50 (both)	SST annual cycles averaged over strong El Niño years
+Niña	50 (both)	SST annual cycles averaged over strong La Niña years
+Niño-Niña	50 (HiRAM only)	SST annual cycles averaged over strong El Niño years minus strong La Niña years
+Niña-Niño	50 (HiRAM only)	SST annual cycles averaged over strong La Niña years minus strong El Niño years

Niño Index (ONI) values greater than +1 (1982, 1986, 1987, 1991, 1994, 1997, 2002, 2009, 2015). The La Niña experiment (+Niña) uses the mean of seven years with ONI values below -1 (1988, 1995, 1998, 1999, 2007, 2010, 2011). Additionally, we analyze two experiments to highlight the contrast between El Niño and La Niña conditions. In the +Nina-Niño (+Nino-Niña) experiment are forced by subtracting the mean SST fields from the nine most active El Niño (seven most active La Niña) years between 1980 and 2015 from the seven most active La Niña (nine most active El Niño) years during that time frame. All aforementioned simulations maintain a constant carbon dioxide concentration, with the exception of the $2\times CO_2$ experiments.

We also analyze multi-ensemble experiments with both models to represent historical TC seasons, described in detail in Levin et al. (2026b). For AM2.5-C360 we generated ten ensemble members, and for HiRAM we generated five ensemble members. Each member was forced with bias-corrected observed monthly SSTs (Chan et al. 2021) from the Hadley Centre Sea Ice and Sea Surface Temperature (HadISST) dataset for the period 1871–2021, and each was initialized with distinct atmospheric conditions while sharing identical SST forcing. Although ensembles of five or ten members are too small to reliably estimate higher-order properties or fit a discrete probability distribution to the simulated TC counts, they provide a large number of additional SST-forced seasonal samples for evaluating the relationship between the ensemble mean and variance. These simulations are therefore used in combination with the idealized experiments with larger ensemble sizes described above and the 1,000-member DL ensemble described below to assess the robustness of the inferred distributional behavior across different models, SST states, and ensemble sizes.

The effects of limited ensemble size are not explicitly corrected for in our analysis. Instead, we assess the sensitivity of our conclusions to ensemble size by separately presenting the relationship between ensemble mean and variance for all available ensembles (Figures 2a and 2b) and for only large ensembles ($n \geq 30$) in Figures 2c and 2d. The latter panels excludes the five- and ten-member historical ensembles, allowing the inferred distributional relationships to be evaluated independently of these smaller ensembles.

In this study, we employ the 1° horizontal resolution DL-based Ai2 Climate Emulator version 2 (ACE2, Watt-Meyer et al. 2025), trained on ERA5 reanalysis (Hersbach et al. 2020), to perform huge ensemble annual simulations of several Atlantic TC seasons. The model, which runs autoregressively to predict a field of atmospheric variables at six-hourly timesteps, is forced by observed HadISST SSTs (Schneider et al. 2013) and by annually varying greenhouse gas concentrations.

Previous studies have demonstrated the physical realism of ACE2-simulated TCs across a range of timescales. Watt-Meyer et al. (2025) showed that ACE2 reproduces the observed geographic distribution of TC tracks across global basins and simulates a realistic annual global TC frequency when compared with TCs identified in ERA5 using the same tracking algorithm. Additionally, Chien et al. (2025) and Levin et al. (2026a) demonstrated that ACE2 captures observed patterns of interannual TC variability across multiple ocean basins. Beyond reproducing TC climatology and variability, recent studies have evaluated whether ACE2 represents TC activity through physically sound mechanisms. Chien et al. (2025) examined the relationship between ACE2-simulated TC genesis and large-scale environmental conditions using the genesis potential index (GPI) of Tippett et al. (2011), which incorporates key environmental controls on TC formation including vertical wind shear, vorticity, column relative humidity, and SSTs. They found that simulated TC genesis occurs preferentially in regions with simulated favorable GPI values, suggesting that ACE2 generates TCs in physically realistic environments. Furthermore, the simulated seasonal cycle of TC genesis closely follows the simulated seasonal evolution of GPI across most basins, indicating that ACE2 captures the annual cycle of TC environmental favorability, although the Atlantic seasonal cycle is somewhat more gradual than observed.

Chien et al. (2025) further evaluated subseasonal TC variability in ACE2 by examining modulation of TC activity by the Madden–Julian Oscillation (MJO) in the model. They found that both TC genesis and GPI anomalies in ACE2 respond consistently with observed MJO-phase-dependent changes, both spatially and when aggregated over ocean basins. These results indicate that ACE2 captures not only the statistical relationship between the MJO and TC activity, but also the associated environmental mechanisms controlling changes in TC genesis across MJO phases. Lastly, Chien et al. (2026) detect a clear relationship between convectively coupled Kelvin waves and simulated TCs in ACE2, one that has challenging to uncover given the limited samples in the observed record. They show this connection is physically-grounded, as favorable changes in the large-scale environment associated with the wave propagation are associated with increases in TC genesis, including increases in atmospheric relative humidity and vorticity. The aforementioned results highlighting ACE2's ability to capture various aspects of global TC activity motivate our use of the model to generate samples from the SST-conditioned Atlanic TC count distribution.

Following the methods of Levin et al. (2026a), we generate 1,000-member ensembles for each year during 2005–2020, as well as for the anomalously inactive 1982 Atlantic TC season. For each target year, ACE2 is integrated repeatedly with prescribed observed SSTs from that year applied as fixed, repeating boundary conditions. For a given target year, the model is run for autoregressively for 100 years under the repeating observed SST forcing. To generate 1,000 ensemble members, this process is repeated 10 times, where each 100-year model integration is initialized from a different atmospheric state, such that each simulated year represents one ensemble member and the ensemble spread represents internal atmospheric variability under identical SST forcing.

b. Data and storm tracking

For the historical record of observed Atlantic TC counts from 1878 to 2024, we utilize the adjusted dataset developed using the methods of Landsea et al. (2010) and assessed in Villarini et al. (2011), where we require that storm maximum wind speeds must exceed 17 m s^{-1} for at least 48 hours.

We follow the approach described in Levin et al. (2026b) to track TCs and seed disturbances in both dynamical models. Specifically, we apply the tracking algorithm of Harris et al. (2016), which identifies candidate storms based on local minima in sea level pressure and applies additional thresholds on vorticity, warm-core structure, wind speed, and duration. Consistent with Villarini et al. (2011), we require all identified TCs to have a minimum lifetime of 72 hours. To track TCs in the ACE2 DL model, we adopt a similar approach following Chien et al. (2025) and Levin et al. (2026b). In this case, we use the TempestExtremes algorithm (Ullrich and Zarzycki 2017), which also detects systems based on local minima in sea level pressure and applies additional constraints on wind speed, duration, location, and warm-core structure.

We acknowledge that two different TC tracking algorithms are used for the two sets of model simulations analyzed in this study: the GFDL physics-based climate models and the ACE2 DL-based climate emulator. Therefore, in addition to differences arising from the model frameworks themselves (i.e., physics-based versus data-driven), differences in simulated TC statistics may also reflect differences in the tracking methodologies. Previous studies have shown that different TC tracking algorithms, can influence TC detection in climate model simulations and contribute to inter-model differences (e.g., Walsh et al. 2007; Horn et al. 2014; Raavi and Walsh 2020). However, we note that the tracking algorithm applied to the GFDL physics-based models (Harris et al. 2016) and the TempestExtremes-based algorithm applied to ACE2 (Ullrich and Zarzycki 2017) share the same general framework for identifying TCs. Specifically, both approaches (1) identify candidate disturbances from local sea-level pressure minima, (2) connect candidate points through time to construct storm trajectories, and (3) apply additional criteria requiring sufficient duration, intensity, and warm-core structure. Thus, despite differences in their implementation, the overall physical definition of a TC is broadly consistent between the two tracking methodologies.

The trackers differ in the order in which they apply the different TC criteria and the specific methods used to quantify each criterion (e.g., definitions of storm intensity and warm-core structure). Although it is difficult to isolate the contribution of the tracking algorithm itself to differences between the model simulations, we consider the tracker to be an integrated component of each modeling framework. Differences in TC tracking represent one model component, analogous to differences in the representation of physical processes, parameterizations, or model architecture. Therefore, our comparisons reflect the combined influence of the model and its associated TC tracking approach.

c. Theoretical TC proxy

As in Levin et al. (2026b) and Levin et al. (2026a), we employ Hsieh et al. (2020)'s probabilistic framework, which decomposes annual TC counts into a precursor seed disturbance phase followed by the phase during which the seed develops into a full TC. Thus, the annual number of Atlantic TCs is assumed to follow a Binomial distribution:

$$N_{TC} \sim \text{binom}(N_s, P), \tag{1}$$

where N_s is the number of seeds and P is the probability that a seed disturbance transitions into a fully developed TC. Consequently, the expected seasonal count of Atlantic TCs N_{TC}, is given by

$$N_{TC} = N_s \times P. \tag{2}$$

In this study, we evaluate the seed–probability framework by using explicitly tracked seed counts to estimate N_s, although the seed proxy developed by Hsieh et al. (2020) has developed a climate-conditioned expectation for seed frequency. Additionally, the probability that a seed develops into a TC (P) is parameterized as a function of the large-scale environmental conditions ($P(\Lambda)$):

$$P \approx P(\Lambda) = \frac{1}{1 + (\Lambda_0/\Lambda)^{1/\gamma}}, \tag{3}$$

where $\Lambda_0 = 0.014$ and $\gamma = -0.9$ are constant dimensionless fitting parameters. These parameters were derived from the logistic regression fit shown in Figure 4 of Tang and Emanuel (2012), which quantifies the likelihood that a seed disturbance intensifies into a TC as a function of the mean environmental ventilation index around that storm. This fit is computed using observed global TC seed data and the ventilation index computed using reanalysis data spanning 1990–2009. These parameters are only fit to the historical period using global data, so they might not be appropriate for use in this study, which only examines Atlantic TCs, some of which form outside of the 1990-2009 period.

$$\Lambda = \frac{v_s \cdot \chi}{PI}, \tag{4}$$

is the ventilation index defined by Tang and Emanuel (2010) and Tang and Emanuel (2012), measuring the degree to which entrainment of low entropy air can limit the storm's intensity. v_s is vertical wind shear, PI is potential intensity, and χ is moist entropy deficit. As in Levin et al. (2026b), We compute the mean Atlantic basin $P(\Lambda)$ over 10–30°N. Following the methodology of Vecchi et al. (2019) and Hsieh et al. (2020), we compute the proxy during the climatologically most active portion of the season, June–November.

3. Results

a. Unprecedentedly large ACE2 historical ensemble

We display the seasonal TC count distributions simulated by the 1,000-member ACE2 historical ensemble in Figure 1, adapted from Figure 2 of Levin et al. (2026a). The ensemble distributions exhibit year-to-year differences in both their central tendency and spread. The total ensemble range (maximum minus minimum TC count) varies considerably, from 11 storms in 1982 to 26 storms in 2012. The ensemble mean and variance for each year are summarized in Table 2, while their relationship is examined in more detail in Section 3b.

The large ensemble size also enables examination of higher-order characteristics of the seasonal distributions beyond their mean and variance. In particular, we quantify the asymmetry of each year's ensemble distribution using the coefficient of skewness (COS),

$$COS = \frac{\sum_{i=1}^{n}(x_i - \bar{x})^3}{ns^3}, \tag{5}$$

where x_i is the seasonal TC count from the ith ensemble member, $\bar{x}$ is the ensemble mean, s is the sample standard deviation, and n = 1,000 is the ensemble size. Positive values of COS indicate a distribution with a longer or heavier right tail, whereas negative values indicate a longer or heavier left tail. A value of zero corresponds to a symmetric distribution.

The coefficient of skewness ranges from 0.10 to 0.48 across the seventeen historical seasons (Table 2), indicating that every ensemble distribution exhibits slight positive skewness. Thus, while most ensemble members cluster around the mean seasonal TC count, each distribution possesses a modest tail toward more active seasons. This behavior is physically reasonable for seasonal TC counts. Because TC counts are bounded below by zero but have no fixed upper

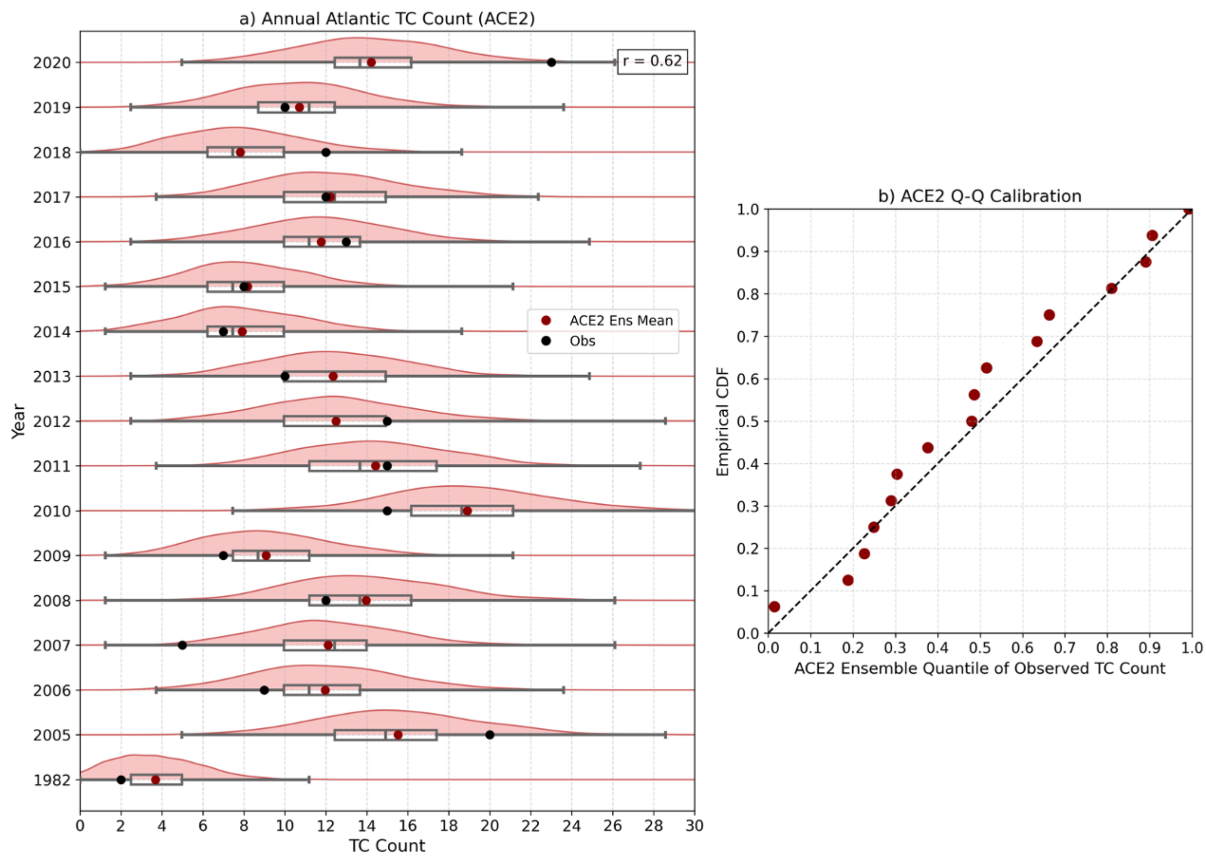

FIG. 1. a) The ACE2 1,000-member ensemble distribution of Atlantic TC counts for 1982 and 2005–2020, shown in red using kernel density estimate (KDE) probability density functions, with the corresponding box-and-whisker plots overlaid in gray. The whiskers denote ensemble minimum and maximum values, the box edges represent 25th and 75th percentiles, and the center line indicates the ensemble median. The red dot denotes ensemble mean, and the black dot represents observed TC count computed using the methods of Landsea et al. (2010). The correlation between the annual ensemble-mean TC count and the observed counts is shown in the upper-right corner. b) Q-Q calibration diagnostic of ACE2 over the 17 years, where each point represents the empirical cumulative distribution of the observed TC count within the corresponding ensemble distribution. A well-calibrated ensemble is indicated by alignment with the dashed 1:1 line. This figure has been adapted from Levin et al. (2026a).

bound, realizations with unusually large numbers of storms can occur more readily than equally extreme low-count realizations, naturally producing a right-skewed distribution. The effect is most pronounced during climatologically inactive years. For example, the 1982 ensemble, which has the lowest mean TC count, exhibits the largest coefficient of skewness (0.48). Since its distribution is centered near only three storms, there is relatively little room for a left tail but considerable room for occasional realizations with substantially higher TC counts. Overall, the consistent, albeit modest, positive skewness across all years suggests that slight right-skewness is a robust characteristic of the ACE2 seasonal TC count distributions.

The ACE2 ensemble exhibits strong calibration to the observed record across multiple metrics. The Q–Q (Quantile-Quantile) calibration diagnostic (Figure 1b) closely follows the 1:1 line, indicating that the observed TC counts verify approximately uniformly across the ensemble distributions. This suggests that, in a probabilistic sense, the model is well calibrated to the observed record. Consistent with the results of the Q–Q plot, the observed TC count lies within the ensemble range for all years considered, and falls within the interquartile range (25th–75th percentile) for eight of the seventeen seasons. Additional ensemble calibration metrics for the 1,000 member ACE2 ensemble are described in Levin et al. (2026a). The correlation between the ensemble-mean and observed TC counts (r = 0.62) further indicates that the model captures a substantial portion of the interannual variability. This retrospective skill is comparable to that of other dynamical and statistical methods (e.g., Vecchi et al. 2014; Zhao et al. 2009).

Despite the overall model calibration, there are notable seasons in which the observed TC count lies in the tails of the ensemble distribution. For example, during the relatively inactive 2007 season (five observed TCs), the ACE2 ensemble distribution is centered around approximately twelve TCs, placing the observation in the lower tail. Conversely, the 2020 season was extremely active (23 observed TCs), while the ensemble distribution is centered near fourteen TCs, with the observed count verifying at the 99.5th percentile (Levin et al. 2026a). This result suggests that the SST boundary conditions could have only been moderately favorable for Atlantic TCs, and that subseasonal variability might have acted on top of such a large-scale environmental state. Refer to Levin et al. (2026a) for a well-calibrated distribution of seasonal TC counts for the 2020 season. Finally, while the kernel density estimates (KDEs) of Figure 1 provide a qualitative visualization of the ensemble distributions, they are not well suited for quantifying dispersion. In the following section, we therefore formally assess the dispersion properties of the ACE2 seasonal TC count distributions and compare them with those from physics-based climate models.

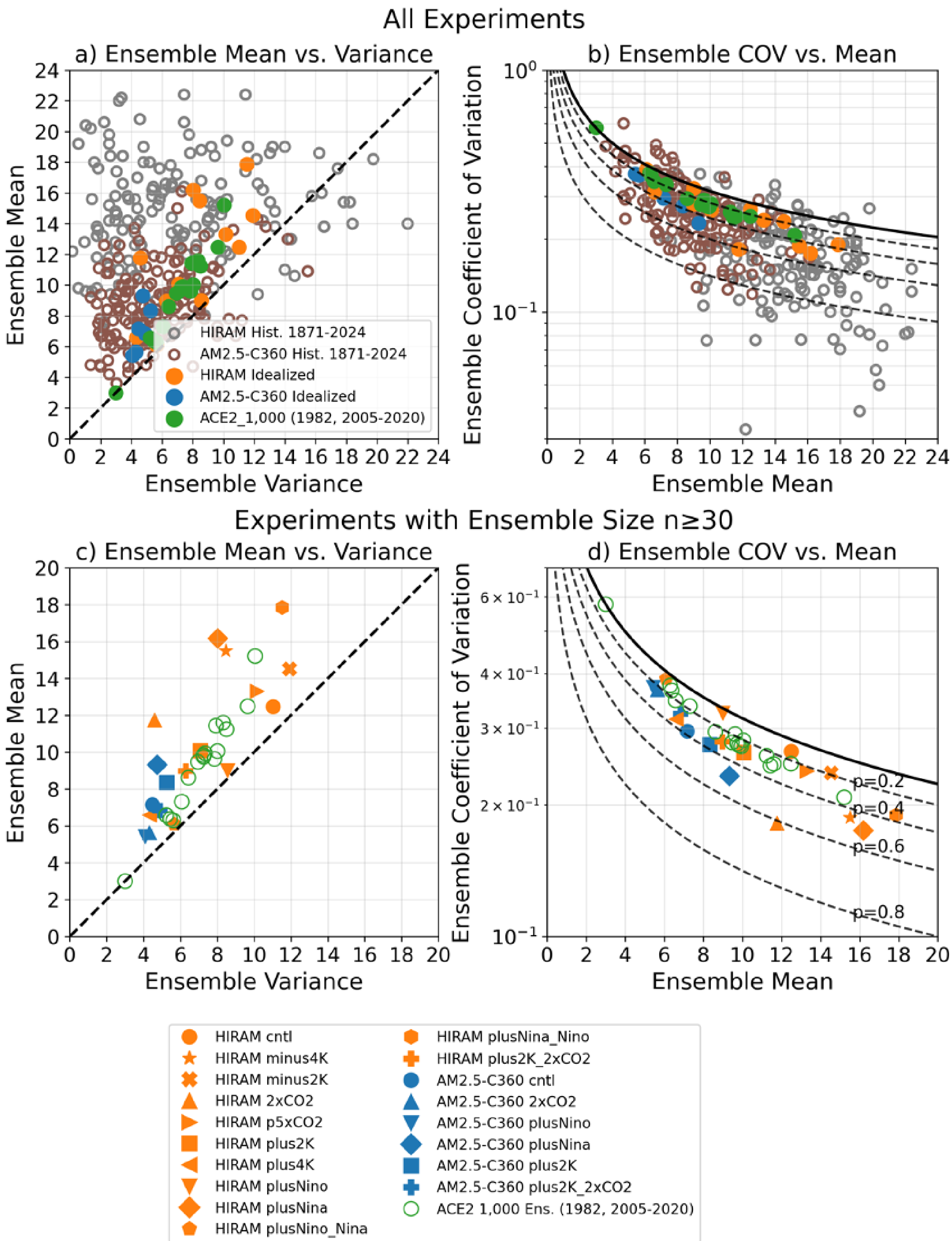

All Experiments
a) Ensemble Mean vs. Variance
b) Ensemble COV vs. Mean
Ensemble Mean
Ensemble Variance
Ensemble Coefficient of Variation
HIRAM Hist. 1871-2024
AM2.5-C360 Hist. 1871-2024
HIRAM Idealized
AM2.5-C360 Idealized
ACE2_1,000 (1982, 2005-2020)
Experiments with Ensemble Size n≥30
c) Ensemble Mean vs. Variance
d) Ensemble COV vs. Mean
p=0.2
p=0.4
p=0.6
p=0.8
HIRAM cntl
HIRAM minus4K
HIRAM minus2K
HIRAM 2xCO2
HIRAM p5xCO2
HIRAM plus2K
HIRAM plus4K
HIRAM plusNino
HIRAM plusNina
HIRAM plusNino_Nina
HIRAM plusNina_Nino
HIRAM plus2K_2xCO2
AM2.5-C360 cntl
AM2.5-C360 2xCO2
AM2.5-C360 plusNino
AM2.5-C360 plusNina
AM2.5-C360 plus2K
AM2.5-C360 plus2K_2xCO2
ACE2 1,000 Ens. (1982, 2005-2020)

FIG. 2. a) Relationship between the ensemble mean and variance of seasonal Atlantic TC counts under identical SST forcing, shown across a suite of models and experiments. Each point corresponds to a single season or experiment and represents the variance–mean pair computed from the ensemble distribution of TC counts. Brown-outlined (gray-outlined) points denote historical AM2.5-C360 (HiRAM) simulations forced with observed SSTs, blue (orange) points indicate idealized experiments from AM2.5-C360 (HiRAM), and green points represent the historical 1,000-member ACE2 ensemble. The black dashed line shows the 1:1 relationship, corresponding to equidispersion. Points below (above) the line indicate underdispersion (overdispersion). b) Relationship between the ensemble mean and the coefficient of variation of seasonal TC counts, using the same models, experiments, and color scheme as in panel (a). The solid black curve indicates the Poisson expectation, $COV = 1/\sqrt{\mu}$, while the dashed black curves indicate the Binomial expectation, $COV = \sqrt{\frac{1-p}{\mu}}$, where p=0.2, 0.4, 0.6, and 0.6, labeled in panel d). c,d) Same as panels (a) and (b), respectively, but excluding the smaller-ensemble historical AM2.5-C360 and HiRAM simulations. Idealized experiments are distinguished by marker shape. Experiments shared across both models (i.e. the 'cntl' experiment) have the same marker shape across both models.

b. Dispersion of simulated conditional TC counts across models

We examine the relationship between the ensemble mean and variance of seasonal Atlantic TC counts under identical boundary forcing in Figures 2a and 2c across a suite of models and experiments. For each season, we compute the ensemble mean and ensemble variance of TC counts subjected to the same prescribed SST forcing, with each point in these figures representing the mean–variance pair associated with a single season.

Across all models and experiments, including both historical and idealized simulations, seasonal TC counts are systematically underdispersed, suggesting the ensemble distributions have less spread than would be diagnosed from a Poisson distribution. This behavior is evident from the fact that most points lie above the 1:1 line, indicating that the ensemble variance is smaller than the ensemble mean for most seasons. The only points lying below the 1:1 line are from the smaller ensemble sized experiments of HiRAM (five members) and AM2.5-C360 (ten members), where the sample variance is less likely to represent the true underlying variance due to the small sample size. Even for those historical experiments, the vast majority of points for HiRAM (141/154) and AM2.5-C360 (145/154) lie above the 1:1 line. Idealized simulations from AM2.5-C360 and HiRAM (Figures 2a and 2c) exhibit this pattern for all experiments. The 1,000-member historical ensemble generated using ACE2 (Figures 2a, 2c and Table 2) also displays pronounced underdispersion, with sixteen of the seventeen examined seasons exhibiting variances lower than their corresponding means, and none showing overdispersion. The remaining season, 1982, is approximately equidispersed, with both the mean and variance near three TCs. This season is exceptionally inactive relative to typical TC seasons and represents an outlier within the ensemble. Taken together across several state-of-the-art climate models with different underlying dynamics, seasonal Atlantic TC activity violates the equidispersion property of the Poisson distribution and provide clear evidence against a simple conditional Poisson process description of seasonal TC counts in these models.

We further find that the relationship between ensemble mean and variance becomes more tightly organized as ensemble size increases. For large ensembles with more than 30 members, as in the ACE2 simulations and AM2.5-C360 and HiRAM idealized experiments shown in Figure 2c, the mean–variance pairs cluster closely around a well-defined curve and remain within a small distance of the 1:1 line. In contrast, the AM2.5-C360 and HiRAM historical ensembles, which contain substantially fewer members (five to ten members), show higher spread in their seasonal data points, with some seasons lying close to the 1:1 line and others lying further away from the 1:1 line. These results stress the high sampling variability of estimating the ensemble variance using small ensemble sizes. The larger ensemble sizes yield more clustered and consistent estimates of the mean-variance relationship between sampled seasonal Atlantic TC count distributions.

In addition to examining the relationship between the ensemble mean and variance, we analyze how the ensemble coefficient of variation (COV) varies with the ensemble mean of seasonal Atlantic TC counts in Figures 2b and 2d. The COV is defined as

$$COV = \frac{\sigma}{\mu}, \tag{6}$$

where σ and μ denote the standard deviation and mean of the distribution, respectively. Throughout this study, these quantities are estimated from the model ensembles using the sample standard deviation, s, and ensemble mean, $\bar{x}$. The COV is a dimensionless measure of dispersion, allowing comparisons among distributions with different average TC activity. Smaller values of COV indicate that the ensemble spread is small relative to the mean, whereas larger values indicate greater relative variability. Examining how COV varies with μ therefore provides insight into how relative model uncertainty changes for seasons with different levels of simulated TC activity.

The expected relationship between COV and μ differs between common discrete count models. For a Poisson distribution, the mean and variance are equal, such that $\mu = \sigma^2 = \lambda$, where λ is the rate parameter. In this case,

$$COV_{\text{Poisson}} = \frac{\sigma}{\mu} = \frac{\sqrt{\mu}}{\mu} = \frac{1}{\sqrt{\mu}}, \tag{7}$$

implying that the coefficient of variation decreases with increasing mean solely due to counting statistics. A decreasing COV with increasing μ is therefore expected under a Poisson process.

For a Binomial distribution describing n independent Bernoulli trials with success probability p, the mean and variance are given by $\mu = np$ and $\sigma^2 = np(1-p)$. The corresponding COV is

$$COV_{\text{Binomial}} = \frac{\sigma}{\mu} = \frac{\sqrt{np(1-p)}}{np} = \sqrt{\frac{1-p}{\mu}}. \tag{8}$$

Both Poisson and Binomial models therefore predict that COV decreases with increasing μ and scales as $1/\sqrt{\mu}$. However, the Binomial distribution includes the additional multiplicative factor $\sqrt{1-p}$, which suppresses COV relative to the Poisson expectation for $0 < p < 1$. Therefore, Binomial distributions have smaller coefficients of variation than Poisson distributions with similar mean values.

We examine the relationship between ensemble COV and ensemble mean μ of seasonal Atlantic TC counts under identical boundary forcing across a suite of models and experiments in Figures 2b and 2d and for the ACE2 1,000 member ensemble in Table 2. For each season, COV and μ are computed from the distribution of TC counts across ensemble members subjected to the same prescribed SST forcing. Each point therefore represents a COV–μ pair associated with a single season. Across all models and experiments, including both historical and idealized simulations, the ensemble COV decreases with increasing ensemble mean: the relative model uncertainty is smaller in seasons with larger simulated activity. While this decreasing trend alone does not distinguish between Poisson and Binomial processes, we find that the majority of COV–μ pairs lie below the Poisson expectation given by $COV = 1/\sqrt{\mu}$. Instead, these points fall within the range predicted by a Binomial framework, as illustrated by the curves corresponding to $COV = \sqrt{(1-p)/\mu}$ for representative values of $p = 0.2, 0.4, 0.6,$ and 0.8. This behavior is evident in both the physics-based AM2.5-C360 and HiRAM simulations and is particularly clear in the 1,000-member historical ensemble generated using the ACE2 model, for which all seasons except 1982 fall below the Poisson curve.

The lower COV relative to the Poisson expectation provides evidence against modeling the SST-conditioned TC count distribution using a Poisson distribution. Instead, these results suggest that the SST-conditioned Atlantic TC count distribution follows a Binomial distribution, where TC genesis is governed by a finite number of seed disturbances and environment-dependent seed-to-TC conversion probabilities. Furthermore, the clustering of points from the larger ensemble simulations within the Binomial expectation curves for p between 0.2 and 0.4 in Figure 2d suggests that this range represents a plausible set of effective seed-to-TC conversion probabilities across the modeled climate states considered here.

Although the experiments across models generally fall within the $0.2 \leq p \leq 0.4$ range in Figure 2d, there remains noticeable spread across different models and experiments. This spread may reflect a combination of sampling uncertainty due to finite ensemble sizes and differences in how each model represents the physical processes controlling TC formation. Previous studies have shown that climate models and their experiments can exhibit different biases in their representation of both the number of precursor seed disturbances (N_s) and the probability that these disturbances develop into TCs (P) (Yang et al. 2021; Hsieh et al. 2022). Consistent with these findings, Figure 2d suggests that different models and experiments may occupy distinct regions of the Binomial parameter space, reflecting differences in their effective representations of N_s and P.

Additional analysis could help determine whether this spread represents true differences in the conditional distribution of TC counts across climate states or uncertainty arising from limited ensemble sampling. In particular, larger ensembles from physics-based climate models would allow more robust estimates of the variance structure and help distinguish systematic model differences from internal variability. Future work could also examine how variations in large-scale environmental controls of TC formation influence the inferred values of N_s and P, providing further insight into additional sources of predictability beyond the SST-forced response examined here.

c. Goodness-of-fit tests for 1,000 member ACE2 ensemble

Next, we examine the seasonal Atlantic TC count distributional properties of the 1,000-member ACE2 historical ensemble. The large ensemble size allows robust statistical inference that is not possible for conventional seasonal prediction systems, which typically include only a few dozen members. We analyze ensemble distributions for each season in the continuous period from 2005 to 2020 and 1982, with summary statistics for each season reported in Table 2. Each row in the table represents properties of the seasonal TC count distribution across the 1,000 ensemble members.

As shown in Figure 2, all sixteen seasons in the 2005-2020 period exhibit ensemble variances that are smaller than their corresponding means, indicating systematic underdispersion and smaller distribution spread than would occur in a Poisson distribution. Variance-to-mean ratios range from 0.69 to 0.84 for these years, while coefficients of variation range from 0.21 to 0.38. The strongest deviation from equidispersion between 2005-2020 occurs in 2010, which has the lowest variance-to-mean ratio and coefficient of variation, while 2018 is closest to equidispersed behavior during this period. This consistent underdispersion demonstrates that the equidispersion property implied by a Poisson process is not supported by the ACE2 ensemble distributions during the 2005-2020 period.

To further assess whether the ACE2 simulated Atlantic seasonal TC count distributions are consistent with a Poisson process, we conduct Monte Carlo experiments. For each season, we generate 10,000 synthetic ensembles by drawing 1,000 samples 10,000 times from a Poisson distribution with rate parameter equal to the ACE2 ensemble-mean TC count for that season. For each synthetic ensemble, we compute the sample variance, yielding a distribution of variances expected under Poisson sampling variability at the given mean.

We illustrate the results for two representative seasons, 2010 and 2018, which span the range of dispersion characteristics in the ACE2 ensemble during the 2005–2020 period (Figure 3). Monte Carlo Poisson simulation results for all seasons are shown in Figure S1. Under the Poisson assumption, the ACE2 ensemble variance for a given season should fall within the distribution of variances generated by these Monte Carlo simulations.

Instead, we find that the ACE2 ensemble variance lies in the extreme left tail of the Monte Carlo distributions for most seasons, indicating substantially reduced ensemble spread relative to Poisson expectations. This behavior is summarized in Figure 3c, which shows the percentile rank

TABLE 2. Characteristics of the seasonal Atlantic TC count distributions derived from a 1,000-member ensemble of the ACE2 historical simulation forced with observed seasonal SSTs. For each season, ensemble mean, variance, variance-to-mean ratio, COV, and COS are shown. Akaike Information Criterion (AIC) scores are computed by fitting the ensemble TC counts to Poisson and Binomial distributions using maximum likelihood estimation and method of moments. We do not include a Binomial fit for the 1982 season, since the estimate of the number of trials $\hat{n}$ in the method of moments estimation is negative, rendering the estimation unphysical. The quantity Δ AIC is defined as the AIC of the Binomial fit minus that of the Poisson fit, such that negative values indicate a preferred Binomial formulation.

Year	Mean	Variance	Variance/Mean	COV	COS	AIC Poisson	AIC Binomial	Δ AIC
1982	2.96	2.97	1.00	0.58	0.48	3863.8	–	–
2005	12.5	9.7	0.78	0.25	0.22	5129.7	5100.7	-29.0
2006	9.6	7.9	0.82	0.29	0.22	4909.9	4892.3	-17.6
2007	9.7	7.3	0.75	0.28	0.28	4851.3	4814.6	-36.7
2008	11.2	8.5	0.76	0.26	0.22	5009.4	4975.9	-33.5
2009	7.3	6.1	0.84	0.34	0.37	4636.1	4622.2	-13.9
2010	15.2	10.1	0.66	0.21	0.21	5217.1	5144.8	-72.3
2011	11.6	8.3	0.72	0.25	0.24	4999.1	4951.9	-47.2
2012	10.1	8.0	0.79	0.28	0.30	4931.1	4909.5	-21.6
2013	9.9	7.3	0.74	0.27	0.10	4874.9	4834.3	-40.6
2014	6.3	5.5	0.87	0.37	0.31	4526.5	4516.8	-9.7
2015	6.6	5.2	0.79	0.35	0.47	4494.1	4472.8	-21.3
2016	9.5	7.0	0.74	0.28	0.18	4817.0	4775.4	-41.6
2017	9.8	7.3	0.74	0.28	0.26	4850.7	4810.9	-39.8
2018	6.3	5.6	0.89	0.38	0.31	4550.3	4545.9	-4.4
2019	8.6	6.4	0.74	0.29	0.24	4730.0	4693.3	-36.7
2020	11.4	7.9	0.69	0.25	0.18	4964.2	4906.6	-57.6

of the ACE2 ensemble variance relative to the corresponding Poisson-based variance distribution for each season. For thirteen of the seventeen seasons analyzed, the ACE2 ensemble variance falls below the minimum variance produced by the Poisson simulations. With the exception of 1982, for the remaining three seasons, the ACE2 ensemble variance lies below the fifth percentile of the Monte Carlo distribution.

These results provide strong evidence that the ACE2 seasonal TC count distributions are systematically underdispersed relative to a Poisson process. In particular, the simulated ensemble variances are not only smaller than the Poisson expectation, but fall outside the range of sampling variability expected under the assumption that the SST-conditioned seasonal Atlantic distribution is a Poisson distribution.

Finally, the large ensemble size allows direct likelihood-based comparison of Poisson and Binomial models using the Akaike Information Criterion (AIC). For the historical simulated ACE2 seasons, we fit the 1,000 ensemble TC counts to both distributions. The Poisson model is fit by setting the rate parameter equal to the sample mean, corresponding to the maximum likelihood and method of moments estimate. For the Binomial model, parameters are estimated using the method of moments, with the conversion probability given by $\hat{p} = 1 - s^2/\bar{x}$ and the number of trials given by $\hat{n} = \bar{x}/\hat{p}$. For each fitted distribution we compute the AIC,

$$AIC = 2k - 2\ln(\hat{L}), \tag{9}$$

where k is the number of free parameters in the model (one for Poisson, two for Binomial), and $\hat{L}$ is the maximum likelihood of the model. Thus, the AIC quantifies the trade-off between goodness of fit and model complexity, allowing an objective comparison between different distributions for sampled ensemble TC counts. Lower AIC values indicate a better data fit to the underlying distribution. AIC values for the ACE2 simulated seasons are listed in Table 2.

Across all ACE2 simulated seasons between 2005 and 2020, the Binomial model yields a lower AIC than the Poisson one, indicating superior explanatory power for the ensemble TC count distributions using a Binomial distribution. While this does not rule out other underdispersed count models for seasonal Atlantic TC count distributions, such as the COM-Poisson or Poisson-Binomial distributions, it demonstrates that the Poisson assumption is not supported by the 2005-2020 ACE2 ensemble data, whereas a Bernoulli-trials framework provides a substantially better description of the simulated seasonal Atlantic TC counts.

Although all seasons from 2005–2020 in the ACE2 historical ensemble exhibit clear underdispersion, characterized by ensemble variances below the fifth percentile of Poisson expectations (Figure 3) and superior goodness-of-fit to a Binomial distribution relative to a Poisson distribution based on AIC (Table 2), the 1982 season represents a notable exception. As shown in Table 2, the simulated TC count distribution for 1982 is approximately equidispersed, with its mean and variance nearly equal. Consistent with this finding, the ensemble variance lies near the 51st percentile of the Monte Carlo Poisson variance distribution, indicating no clear deviation from a Poisson

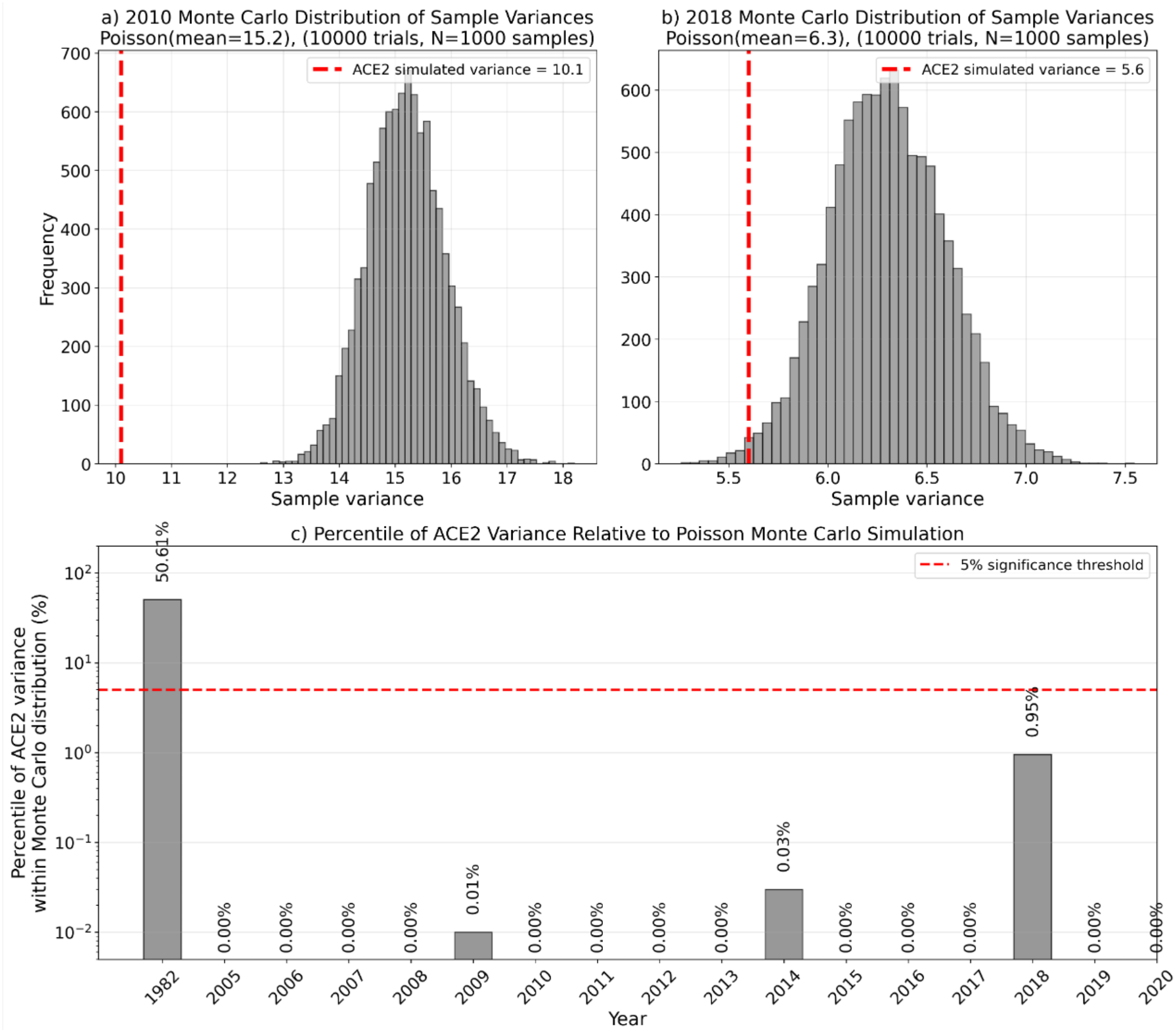

FIG. 3. Monte Carlo assessment of the Poisson assumption for seasonal TC counts using the 1,000-member ACE2 ensemble, shown for 2010 and 2018 (panels a, and b, respectively). Each panel depicts a Monte Carlo simulation of a Poisson with a rate parameter equal to the ensemble mean of the ACE2 1,000-member ensemble simulated year. For each 2010 and 2018 simulated ACE2 season, we generate 1,000 samples from such a Poisson distribution and repeat this process 10,000 times. Then, we find the variance for each group of 1,000 samples from this Poisson distribution, which represents the variance for a theoretical Poisson conditional seasonal Atlantic TC count distribution. The histograms show the distribution of the 10,000 sampled variances for each simulated season, and the vertical dashed line represents the true simulated 1,000-member ensemble variance from the ACE2 model. The verified quantile of the simulated variance across the histogram is shown in the upper right portion of each panel. Monte Carlo distributions for all remaining years (1982, 2005–2020) are provided in Figure S1. Panel (c) depicts the verified quantile in the histogram of the simulated variance for all years (1982, 2005–2020) on a logarithmic scale The red dashed horizontal line marks the 5% significance threshold.

distribution. Furthermore, because the ensemble variance slightly exceeds the mean, the Binomial distribution cannot be fit: the estimate of the number of trials $\hat{n}$ becomes negative, yielding an unphysical parameterization. The Poisson distribution yields the lowest AIC score for 1982 across all years considered, further supporting the interpretation that this season's conditional TC count distribution is equidispersed.

We interpret 1982 as an outlier within both the observational record and the modeled ensemble. According to the observational dataset of Landsea et al. (2010), 1982 is the least active Atlantic TC season in the satellite era, with only two observed storms. This inactive environment likely limits the ability to robustly characterize a range of possible TC counts. Additionally, because the minimum possible seasonal TC count is zero, when the distribution mean of the simulated distribution is very low, the distribution variance approaches zero as well, making dispersion properties difficult to diagnose. In this regime, the distinction between different discrete distributions becomes less pronounced, and equidispersion can arise naturally due to the low count.

Importantly, the presence of other relatively inactive seasons within the ACE2 analysis period, such as 2007, which also exhibits low observed activity of five storms, does not lead to similar behavior. These still show underdispersion in their TC count distributions and favor a Binomial distribution over a Poisson distribution. This indicates that low activity alone does not suggest a Poisson distribution better represents the SST-conditioned TC count distribution. These results suggest that the equidispersed behavior in 1982 reflects the uniquely extreme and unfavorable environmental conditions of that season, rather than a breakdown of our broader conclusions. Across all other seasons analyzed, the ACE2 1,000-member ensembles consistently support the conclusion that seasonal TC counts are not well described by a Poisson process, but are more appropriately represented by a Binomial distribution.

d. Physical basis for the Binomial TC framework

The results presented thus far provide strong evidence against describing seasonal TC counts as a Poisson process. They instead motivate consideration of alternative generative frameworks in which TC formation is more constrained than implied by purely random arrivals. Here, we present empirical support for a finite-opportunity or Binomial framework for tropical cyclogenesis, following the conceptual model proposed by Hsieh et al. (2020); in this framework, seasonal TC counts are interpreted as the number of successful TC formations arising from a finite number of seed disturbances, with the probability of each seed developing into a TC governed by large-scale environmental conditions.

Figure 4 illustrates the ensemble-mean relationships among simulated seasonal TC counts, the Binomial proxy defined as the product of seed count and conversion probability (Seeds $\times P(\Lambda)$), the individual components of this proxy, and the relationship between seed count and conversion probability. Across both models, we find moderate to strong positive correlations between seasonal TC counts and each component of the Binomial framework. In AM2.5-C360, TC counts are more strongly correlated with seed count than with conversion probability ($r = 0.73$ versus $r = 0.53$), whereas in HiRAM the opposite is true, with TC counts more strongly correlated with conversion probability than with seed count ($r = 0.83$ versus $r = 0.62$). Despite these differences, the correlation between the full Binomial proxy (Seeds $\times P(\Lambda)$) and simulated TC counts is strongly positive in both models ($r = 0.76$ for AM2.5-C360 and $r = 0.81$ for HiRAM), indicating that the combined influence of seeds and environmental favorability provides a robust predictor of seasonal TC activity.

We further note that seed count and conversion probability are not independent variables, but instead exhibit moderate positive covariance in both models ($r = 0.43$ for AM2.5-C360 and $r = 0.54$ for HiRAM), consistent with previous findings (Levin et al. 2026b). This covariance suggests that environmental conditions conducive to TC formation may simultaneously influence both the number of precursor disturbances and their likelihood of development. Although the high-resolution atmospheric models used in this study explicitly simulate TC-like vortices, they do not fully resolve all aspects of TC dynamics, including convective-scale processes and inner-core structure. Therefore, the relationship between environmental controls of seed formation and conversion probability may depend on how each model represents the TC intensity spectrum. This caveat is particularly relevant for HiRAM, whose lower horizontal resolution limits its ability to simulate the most intense hurricanes compared with AM2.5-C360. Consequently, the simulated covariance between seed frequency and conversion probability can reflect model-specific representations of TC genesis and intensification. Future work using higher resolution models will be needed to further evaluate whether this relationship is consistent for the most intense storms.

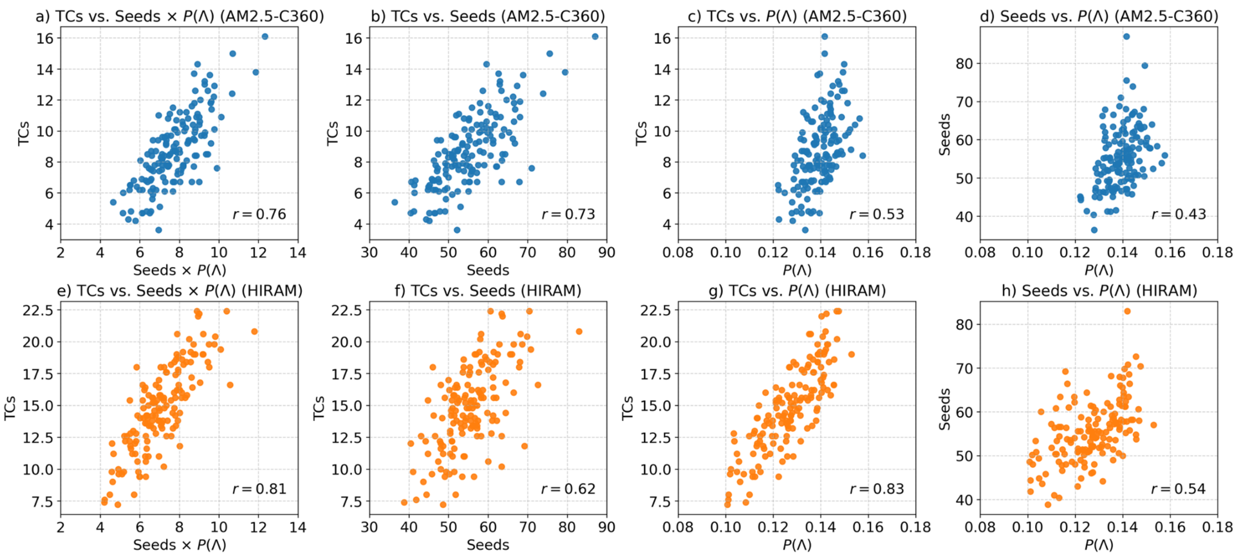

FIG. 4. Scatter plots illustrating relationships between ensemble-mean TC counts, precursor disturbances, and conversion probability in historical atmosphere-only simulations forced with observed SSTs during 1871–2021. Panels (a,e) show ensemble-mean TC count versus the ensemble-mean approximated TC count, defined as the product of seed count and parametrized conversion probability (Seeds $\times P(\Lambda)$). Panels (b,f) show ensemble-mean TC count versus ensemble-mean seed count. Panels (c,g) show ensemble-mean TC count versus ensemble-mean parametrized conversion probability $P(\Lambda)$. Panels (d,h) show ensemble-mean seed count versus ensemble-mean parametrized conversion probability. Top panels correspond to the AM2.5-C360 model (blue), and bottom panels correspond to the HiRAM model (orange). Correlation coefficients are reported in the lower-right corner of each panel.

Taken together, the relationships shown in Figure 4 across both models with different resolutions and convection parameterizations are consistent with a generative picture in which seasonal TC counts arise from a finite number of seeds whose conversion probability depends on the large-scale environment, rather than from an unbounded Poisson process. However, in spite of this colinearity, seeds and genesis probability together provide better explanatory power of seasonal TC frequency, as has also been found in other contexts and models (Vecchi et al. 2019; Hsieh et al. 2020; Yang et al. 2021; Levin et al. 2026b): seasonal TC frequency arises from the probability genesis from a finite set of trials (seeds), where such genesis probability and seed count are climate dependent.

e. Analysis of observational record

The controlled large-ensemble modeling frameworks used in this study allow us to directly estimate the distribution of possible seasonal Atlantic TC counts under a fixed large-scale climate state by holding SST boundary conditions constant across ensemble members. In contrast, the observational record provides only one realization from each TC season. Therefore, while observations can be used to estimate the total variance of the SST-conditioned Atlantic TC count distribution, they cannot directly isolate the variability associated with subseasonal variability from intraseasonal climate variability.

Conceptually, the total interannual variance in observed seasonal TC counts can be decomposed as

$$\sigma^2_{\text{total}} = \sigma^2_{\text{noise}} + \sigma^2_{\text{climate}}, \tag{10}$$

where σ^2_{total} represents the total variance in seasonal TC counts across years, σ^2_{noise} represents the variance of possible seasonal outcomes under a fixed climate state (i.e., the conditional distribution), and $\sigma^2_{\text{climate}}$ represents variance associated with year-to-year changes in the large-scale environment, such as SST patterns.

Because the observational record includes only one seasonal outcome each year, the variance calculated directly from TC counts across the entire observational record estimates σ^2_{total}, not σ^2_{noise} or $\sigma^2_{\text{climate}}$.

To quantify σ^2_{total} in the observed record, we compute the variance of observed annual Atlantic TC counts derived using the methodology of Landsea et al. (2010) and shown in Figure S2. We examine both the full observational record (1878–2024) and the satellite-era record (1980–2024), when TC observations are more reliable. Across both observational subsets, σ^2_{total} ranges from approximately thirteen to fourteen TCs^2, while the mean annual TC count is approximately ten storms (Table 3). Therefore, if the observed record is interpreted as a single unconditioned distribution, seasonal Atlantic TC counts appear overdispersed, with variance exceeding the mean. This would suggest that the distribution of TC counts across different climate states may be better represented by an overdispersed count model, such as a Negative Binomial distribution.

However, this interpretation does not describe the quantity σ^2_{noise}, which relevant when controlling for different climate states across seasons and when making seasonal predictions. Statistical and statistical-dynamical frameworks seek to estimate the distribution of possible outcomes conditioned on a known or forecasted large-scale environment (e.g., Elsner and Jagger 2004, 2006; Jagger and Elsner 2010; Vecchi et al. 2011; Villarini et al. 2012; Davis et al. 2015; Murakami et al. 2016a). Therefore, the relevant quantity to this approach is σ^2_{noise}, not σ^2_{total}. Assuming $\sigma^2_{\text{noise}} \approx \sigma^2_{\text{total}}$ would incorrectly attribute all observed variability to stochastic weather variability within a fixed climate state. Since we assume $\sigma^2_{\text{climate}} > 0$, this approximation would overestimate the SST-conditioned seasonal Atlantic TC count distribution variance. Therefore, using σ^2_{total} to select a conditional discrete count distribution for a statistical framework could incorrectly result in using a overdispersed distribution that overestimates the range of possible seasonal Atlantic TC counts.

Controlled modeling frameworks using large ensembles provide a method for separating the two sources of variability. In this study, estimates of σ^2_{noise} for past observed seasons are obtained from ensembles initialized under identical observed SST boundary conditions by computing the variance of the ensemble distribution. These estimates are shown in the third column of Table 2 for the 1,000-member ACE2 DL ensemble forced with observed SSTs (1982 and 2005–2020), and in Figure 2a for the historical GFDL AM2.5-C360 and HiRAM simulations forced with observed SSTs. The idealized SST perturbation experiments also provide estimates of conditional variability, although these experiments sample artificially constructed climate states and therefore should not be interpreted as direct estimates of observed σ^2_{noise}.

Large ensembles can also provide estimates of $\sigma^2_{\text{climate}}$ by examining variability in the ensemble mean response across different climate states. We estimate $\sigma^2_{\text{climate}}$ using the ACE2 1,000-member ensemble because its large ensemble size provides a more robust estimate of the forced response than the smaller AM2.5-C360 and HiRAM historical ensembles (ten and five members, respectively). Specifically, we compute the variance across annual ACE2 ensemble-mean TC counts (the values shown in the second column of Table 2). This gives an estimate of $\sigma^2_{\text{climate}}$ of approximatly eight TCs^2 (Table 3). Combining this estimate with the observed σ^2_{total} suggests a residual estimate of σ^2_{noise} of approximately six TCs^2. However, this residual estimate should be interpreted cautiously because σ^2_{noise} itself varies with the climate state, as demonstrated by the year-to-year differences in ensemble spread shown in Figure 2 and Table 2.

TABLE 3. Estimates of variance components in historical seasonal Atlantic TC counts. The Observed record provides an estimate of the total interannual variance (σ^2_{total}), computed as the variance of annual TC counts across the record. The $\sigma^2_{\text{climate}}$ is estimated from the ACE2 1,000-member ensemble as the variance of annual ensemble-mean TC counts across different simulated seasons. Results are shown using all available years and more recent years with improved observational techniques. Observed TC counts are derived following Landsea et al. (2010).

Record	Variable	Value
Obs (1878–2024)	Mean	9.5
	σ^2_{total}	14.2
Obs (1980–2024)	Mean	10.2
	σ^2_{total}	13.1
ACE2 (1982, 2005–2020)	$\sigma^2_{\text{climate}}$	7.6

This observational analysis highlights two important points. First, although the unconditioned observed distribution of seasonal Atlantic TC counts appears overdispersed, this does not imply that the SST-conditioned distribution relevant for seasonal prediction is also overdispersed. The observed record alone cannot separate σ^2_{noise} from $\sigma^2_{\text{climate}}$. Second, large ensembles used within controlled modeling frameworks allow us to estimate the conditional TC count distribution because they explicitly separate stochastic internal variability under fixed boundary conditions from variability associated with changes in the climate state. Therefore, the consistent underdispersion relative to a Poisson distribution found across the physics-based models, idealized experiments, and ACE2 DL emulator using different TC tracking techniques suggests that underdispersion is a robust feature of the modeled SST-conditioned TC genesis process. The observational analysis presented here should be viewed as illustrating the limitations of using the single-realization observed record to infer the conditional distribution of seasonal TC activity.

4. Discussion and conclusions

This study provides the first systematic evaluation of the Poisson equidispersion assumption for the conditional seasonal Atlantic TC count distribution using large ensembles from state-of-the-art atmosphere-only models. By leveraging ensembles from both physics-based models (AM2.5-C360 and HiRAM) and a 1,000-member ensemble generated by the DL-based climate emulator ACE2 that use different TC tracking algorithms, we robustly characterize the distributional properties of seasonal TC counts under identical boundary forcing across multiple modeling frameworks without imposing any apriori assumptions about the underlying conditional count distribution. We analyze simulations forced by observed SSTs as well as a suite of idealized SST perturbation experiments, allowing us to examine a broad range of climate states and isolate the role of internal atmospheric variability in shaping the ensemble distribution of seasonal Atlantic TC activity. Across these experiments, we investigate the relationship between the ensemble mean and variance and find that underdispersion is a robust feature of simulated seasonal TC counts. This result is particularly evident in the idealized SST experiments with at least 30 ensemble members, where every experiment across both AM2.5-C360 and HiRAM produces an ensemble variance smaller than the ensemble mean. Although these idealized SST configurations do not necessarily represent realistic climate states, they span a wide range of large-scale environments and consistently support the conclusion that the conditional distribution of seasonal TC counts is underdispersed. These findings indicate that seasonal TC frequency is better represented as a multi-stage process involving a finite number of opportunities for TC formation, consistent with recent physically based arguments (Hsieh et al. 2020).

Several independent lines of evidence support a finite-opportunity interpretation of TC genesis rather than a Poisson process. First, seasonal TC count distributions are systematically underdispersed, with ensemble variances smaller than ensemble means across nearly all seasons, experiments, and modeling frameworks examined. Second, the relationship between the coefficient of variation and ensemble mean deviates from the theoretical Poisson expectation, with relative uncertainty decreasing more rapidly during more active simulated seasons than would be expected from a Poisson process. Third, Monte Carlo experiments demonstrate that the observed ensemble variances are unlikely to arise from finite sampling of an underlying Poisson distribution. Fourth, likelihood-based model comparisons using AIC show that a Binomial distribution provides a better fit than a Poisson distribution to seasonal TC count distributions from the 1,000-member ACE2 ensemble for nearly all seasons analyzed. Finally, diagnostics separating precursor disturbances from the environmental probability of transition to a TC provide a physical basis for a Binomial framework, in which seasonal TC frequency emerges from a finite number of potential disturbances that each have some probability of developing into a TC. This interpretation is consistent with previous studies emphasizing the importance of both disturbance frequency and large-scale environmental controls on TC genesis (Vecchi et al. 2019; Hsieh et al. 2020; Sugi et al. 2020; Yang et al. 2021; Levin et al. 2026b).

These results, implying that simulated TC activity is more constrained than implied by a Poisson process have important implications:

- **Statistical modeling of TCs**: Poisson-based formulations may systematically overestimate uncertainty and misrepresent dispersion structure for seasonal Atlantic TC count SST-conditioned distributions, especially in active seasons. Alternative underdispersed count models, including Binomial, Poisson-Binomial, or related formulations, may provide more physically consistent representations of seasonal TC variability.

- **TC forecasting**: Traditional seasonal Atlantic TC forecasting systems typically provide qualitative forecasts of TC counts, predicting a range of possible storm counts with a confidence percentage in the forecast. This study seeks to improve seasonal TC outlooks by making them more quantitatively robust and providing an approach and interpretation to understand the confidence in such prediction. First, using the proper seasonal Atlantic TC count conditional distribution to model the range of plausible outcomes enables a probabilistic quantification for any possible TC level, including the extreme tail seasons. Additionally, the results from Figures 2b and 2d, showing a systematic decrease in the conditional TC count distribution spread for more active seasons suggest that the conditional distribution variance, and thus confidence in the forecasted TC count, changes depending on the mean TC signal. Therefore, seasons with largely favorable SST boundary conditions for an active season could have more tightly constrained conditional TC count distributions, and thus yield more confident seasonal TC forecasts.

- **Seasonal Atlantic TC predictability**: The systematic underdispersion of the SST-conditioned TC count distribution suggests that the large-scale environmental state constrains seasonal Atlantic TC activity more tightly than has generally been assumed under the canonical Poisson framework. Since the conditional distribution of seasonal TC activity is narrower than previously assumed, SST boundary conditions contain more information about the realized seasonal outcome, implying greater intrinsic predictability of seasonal Atlantic TC outcomes once the large-scale environment is specified. This conclusion is consistent with many skillful seasonal Atlantic TC predictions (Chen and Lin 2011; Vecchi et al. 2014; Murakami et al. 2016b; Klotzbach et al. 2019; Murakami et al. 2025), while providing a physical explanation for why those forecasts exhibit substantial skill.

- **Physical interpretability**: The results reinforce the view that TC counts are controlled by the joint behavior of precursor disturbances (seeds) and environmental conversion probability, rather than by purely random arrivals. Additionally, the Binomial framework offers a physical mechanism for why the TC count distribution coefficient of variation decreases with the distribution mean (Figures 2b and 2d), thus the models exhibit less uncertainty for more active seasons:

    1. For a Binomial distribution, the COV is given by

    $$\mathrm{COV} = \sqrt{\frac{1-p}{np}}.$$

    When the conversion probability p is held fixed, the COV decreases as $1/\sqrt{n}$. Consequently, when a basin experiences a large number of trials or seed disturbances, the relative spread in total TC counts across the ensemble is reduced. This behavior reflects a law-of-large-numbers effect: as the number of trials increases, the total number of successes becomes more consistent. Thus, in seasons with abundant seeds (n), the realized TC counts are intrinsically less variable.

    2. A complementary interpretation involves variations in the conversion probability p. As shown in Figures 4c and 4g, more active seasons are associated with enhanced environmental favorability, reflected in higher values of $P(\Lambda)$. As p increases, the numerator of the COV expression ($\sqrt{1-p}$) decreases, driving the TC count distribution toward increasingly deterministic outcomes. For example, a conversion probability of $p = 0.99$ yields a substantially smaller COV than $p = 0.5$. In highly favorable environments, in addition to more seeds being present, nearly every viable seed develops into a storm, leading to stronger agreement across ensemble members in their simulated TC activity.

- **Role of AI models**: This study highlights the unique role of AI-based climate models in enabling statistical diagnostics that were previously infeasible. The ability to generate ensembles with thousands of members allows robust estimation of dispersion properties and formal goodness-of-fit testing for discrete count distributions, opening new opportunities to re-examine long-standing statistical assumptions in climate science. At the same time, interpreting these AI-driven results relies critically on a strong understanding of the underlying physical processes governing storms, the large-scale climate, and their interactions. Together, this highlights the importance of integrating physical insight with advanced statistical and computational approaches.

One caveat of this study is that it focuses exclusively on seasonal Atlantic TC counts, a basin for which Poisson-based statistical models have been widely applied (e.g., Elsner and Jagger 2004, 2006; Jagger and Elsner 2010; Villarini et al. 2012; Davis et al. 2015; Murakami et al. 2016a). Preliminary analysis suggests that qualitatively similar underdispersion in the ensemble spread of modeled seasonal TC activity is also present in the western North Pacific; however, a quantitative assessment of whether Poisson or Binomial frameworks provide an appropriate description of seasonal TC counts in that basin is beyond the scope of this study. Future work should therefore examine the dispersion properties of the environmentally-conditioned seasonal TC count distribution across additional basins. This includes an evaluation of the proper discrete count distribution, such as the Binomial or Poisson distributions for other basins' TC count conditional distribution.

Another intrinsic caveat of this study, given our use of atmosphere-only models with prescribed SST boundary conditions, is that our experiments do not explicitly represent coupled atmosphere–ocean interactions that are important for TC development. While we acknowledge that air–sea feedbacks play a critical role in TC evolution, isolating the component of internal atmospheric variability that is independent of boundary forcing (i.e., the conditional variance of seasonal TC counts) requires fixing the SST boundary conditions. Therefore, the experimental design used in this study would not be possible in a fully coupled framework. However, because SSTs govern TCs and their large-scale environmental controls, future work could extend this analysis by examining the conditional distribution of seasonal Atlantic TC counts in coupled climate models that include atmosphere-ocean interactions using large ensembles of nudged experiments.

Finally, our results do not assess model accuracy or forecast skill. Several seasons, including 2007 and 2020, lie in the extreme tails of the model-simulated TC count distributions (Figure 1), indicating that accurate prediction of individual seasons remains challenging. As discussed in Levin et al. (2026a), and expected from the intrinsically probabilistic nature of seasonal TC information (e.g., Vecchi and Villarini 2014; Vecchi et al. 2014), such discrepancies may arise from the unpredictability of subseasonal atmospheric variability rather than model limitations. Our findings instead clarify how climate models generate distributions of possible seasonal Atlantic TC counts and provide a physically grounded interpretation of their dispersion properties.

Overall, this work demonstrates the value of combining physics-based and DL–based climate models to rigorously test foundational statistical assumptions. By showing that seasonal TC counts in climate models are underdispersed and more constrained than implied by Poisson randomness, we motivate the development of more physically grounded statistical frameworks for seasonal TC prediction and risk assessment.

Acknowledgments. We thank Professor Libby Barnes, Professor Greg Hakim, and Professor Peter Huybers for helpful discussions and comments, and we thank Dr. Spencer Clark at Ai2, Dr. Mu-Ting Chien at Boston University, and Dr. Colm Talbot and Dr. Mattie Niznik at Princeton Research Computing for their assistance in running the ACE2 model. This work has been supported by the Carbon Mitigation Initiative at Princeton University, funded by BP. E.L. was supported by the National Science Foundation Graduate Research Fellowship. This work was funded, in part, by the Heising-Simons Foundation Grant 2023-4720. The simulations were performed on computational resources managed and supported by Princeton Research Computing, a consortium of groups including the Princeton Institute for Computational Science and Engineering, the Office of Information Technology's High Performance Computing Center, and the Visualization Laboratory at Princeton University.

Data availability statement. Source code of the HiRAM model is available from `https://www.gfdl.noaa.gov/hiram-quickstart`, and the source code of the ACE2 model is available from `https://github.com/ai2cm/ace`. The code to run one year's 1,000-member ensemble and process the output, and track TCs is available at `https://github.com/emmalevin/ACE2_1000`. TC track data and monthly mean environmental conditions generated from the ACE2 1,000 member ensemble are available at the Zenodo repository: `https://doi.org/10.5281/zenodo.19456833` (Levin 2026).

References

Bi, K., L. Xie, H. Zhang, X. Chen, X. Gu, and Q. Tian, 2023: Accurate medium-range global weather forecasting with 3D neural networks. *Nature*, **619 (7970)**, 533–538, https://doi.org/10.1038/s41586-023-06185-3.

Blitzstein, J. K., and J. Hwang, 2014: *Introduction to Probability*. 1st ed., Texts in Statistical Science, Chapman and Hall/CRC, Boca Raton, FL.

Bretherton, C. S., J. R. McCaa, and H. Grenier, 2004: A new parameterization for shallow cumulus convection and its application to marine subtropical cloud-topped boundary layers. Part I: Description and 1D results. *Monthly Weather Review*, **132 (4)**, 864–882, https://doi.org/10.1175/1520-0493(2004)132⟨0864:ANPFSC⟩2.0.CO;2.

Chan, D., G. A. Vecchi, W. Yang, and P. Huybers, 2021: Improved simulation of 19th- and 20th-century North Atlantic hurricane frequency after correcting historical sea surface temperatures. *Science Advances*, **7 (26)**, eabg6931, https://doi.org/10.1126/sciadv.abg6931.

Chen, J.-H., and S.-J. Lin, 2011: The remarkable predictability of interannual variability of Atlantic hurricanes during the past decade. *Geophysical Research Letters*, **38 (11)**, L11 804, https://doi.org/10.1029/2011GL047629.

Chen, J.-H., and S.-J. Lin, 2013: Seasonal predictions of tropical cyclones using a 25-km-resolution general circulation model. *Journal of Climate*, **26 (2)**, 531–543, https://doi.org/10.1175/JCLI-D-12-00061.1.

Chen, L., X. Zhong, F. Zhang, Y. Cheng, Y. Xu, Y. Qi, and H. Li, 2023: Fuxi: A cascade machine learning forecasting system for 15-day global weather forecast. *npj Climate and Atmospheric Science*, **6 (1)**, 190, https://doi.org/10.1038/s41612-023-00512-1.

Chien, M.-T., E. A. Barnes, and E. D. Maloney, 2025: Modulation of tropical cyclogenesis on subseasonal-to-interannual timescales in the deep-learning climate emulator ACE2. *Machine Learning: Earth*, **1 (1)**, 015 008, https://doi.org/10.1088/3049-4753/adfd61.

Chien, M.-T., E. A. Barnes, and E. D. Maloney, 2026: Modulation of tropical cyclogenesis by the convectively coupled Kelvin Waves: Insights from data-driven climate emulator ACE2. *Geophysical Research Letters*, **53**, e2025GL117 387, https://doi.org/10.1029/2025GL117387.

Davis, K., X. Zeng, and E. A. Ritchie, 2015: A new statistical model for predicting seasonal North Atlantic hurricane activity. *Weather and Forecasting*, **30 (3)**, 633–647, https://doi.org/10.1175/WAF-D-14-00156.1.

Elsner, J. B., and T. H. Jagger, 2004: A hierarchical Bayesian approach to seasonal hurricane modeling. *Journal of Climate*, **17 (14)**, 2813–2824, https://doi.org/10.1175/1520-0442(2004)017⟨2813:AHBATS⟩2.0.CO;2.

Elsner, J. B., and T. H. Jagger, 2006: Prediction models for annual U.S. hurricane counts. *Journal of Climate*, **19 (12)**, 2935–2952, https://doi.org/10.1175/JCLI3729.1.

Eusebi, R., W. Yang, G. A. Vecchi, and S. Fueglistaler, 2025: Statistical modeling of North Atlantic hurricane frequency and the impact and role of patterned warming. *Journal of Climate*, **38 (19)**, 5391–5410, https://doi.org/10.1175/JCLI-D-24-0647.1.

Gray, W. M., 1984: Atlantic seasonal hurricane frequency. Part II: Forecasting its variability. *Monthly Weather Review*, **112 (9)**, 1669–1683, https://doi.org/10.1175/1520-0493(1984)112⟨1669:ASHFPI⟩2.0.CO;2.

Gray, W. M., C. W. Landsea, J. Mielke, Paul W., and K. J. Berry, 1992: Predicting Atlantic seasonal hurricane activity 6–11 months in advance. *Weather and Forecasting*, **7 (3)**, 440–455, https://doi.org/10.1175/1520-0434(1992)007⟨0440:PASHAM⟩2.0.CO;2.

Harris, L. M., S.-J. Lin, and C. Tu, 2016: High-resolution climate simulations using GFDL HiRAM with a stretched global grid. *Journal of Climate*, **29 (11)**, 4293–4314, https://doi.org/10.1175/JCLI-D-15-0389.1.

Hersbach, H., and Coauthors, 2020: The ERA5 global reanalysis. **146 (730)**, 1999–2049, https://doi.org/10.1002/qj.3803.

Horn, M., and Coauthors, 2014: Tracking scheme dependence of simulated tropical cyclone response to idealized climate simulations. *Journal of Climate*, **27 (24)**, 9197–9213, https://doi.org/10.1175/JCLI-D-14-00200.1.

Hsieh, T.-L., G. A. Vecchi, W. Yang, I. M. Held, and S. T. Garner, 2020: Large-scale control on the frequency of tropical cyclones and seeds: a consistent relationship across a hierarchy of global atmospheric models. *Climate Dynamics*, **55 (11)**, 3177–3196, https://doi.org/10.1007/s00382-020-05446-5.

Hsieh, T.-L., W. Yang, G. A. Vecchi, and M. Zhao, 2022: Model spread in the tropical cyclone frequency and seed propensity index across global warming and ENSO-like perturbations. *Geophysical Research Letters*, **49 (7)**, e2021GL097 157, https://doi.org/10.1029/2021GL097157.

Hsieh, T.-L., B. Zhang, W. Yang, G. A. Vecchi, M. Zhao, B. J. Soden, and C. Wang, 2023: The influence of large-scale radiation anomalies on tropical cyclone frequency. *Journal of Climate*, **36 (16)**, 5431–5441, https://doi.org/10.1175/JCLI-D-22-0449.1.

Jagger, T. H., and J. B. Elsner, 2010: A consensus model for seasonal hurricane prediction. *Journal of Climate*, **23 (22)**, 6100–6113, https://doi.org/10.1175/2010JCLI3686.1.

Johnson, N. L., A. W. Kemp, and S. Kotz, 2005: *Univariate Discrete Distributions*. 3rd ed., Wiley Series in Probability and Statistics, Wiley, Hoboken, NJ.

Klotzbach, P., and Coauthors, 2019: Seasonal tropical cyclone forecasting. *Tropical Cyclone Research and Review*, **8 (3)**, 134–149, https://doi.org/10.1016/j.tcrr.2019.07.001.

Klotzbach, P. J., S. G. Bowen, R. Pielke, and M. Bell, 2018: Continental U.S. hurricane landfall frequency and associated damage: Observations and future risks. *Bulletin of the American Meteorological Society*, **99 (7)**, 1359–1376, https://doi.org/10.1175/BAMS-D-17-0184.1.

Kochkov, D., and Coauthors, 2024: Neural general circulation models for weather and climate. *Nature*, **632 (8027)**, 1060–1066, https://doi.org/10.1038/s41586-024-07744-y.

Kortum, G., G. A. Vecchi, T.-L. Hsieh, and W. Yang, 2024: Influence of weather and climate on multidecadal trends in Atlantic hurricane genesis and tracks. *Journal of Climate*, **37 (5)**, 1501–1522, https://doi.org/10.1175/JCLI-D-23-0088.1.

Lam, R., and Coauthors, 2023: Learning skillful medium-range global weather forecasting. *Science*, **382 (6677)**, 1416–1421, https://doi.org/10.1126/science.adi2336.

Landsea, C. W., G. A. Vecchi, L. Bengtsson, and T. R. Knutson, 2010: Impact of duration thresholds on Atlantic tropical cyclone counts. *Journal of Climate*, **23 (10)**, 2508–2519, https://doi.org/10.1175/2009JCLI3034.1.

Lang, S., and Coauthors, 2024: AIFS: ECMWF's data-driven forecasting system. URL https://arxiv.org/abs/2406.01465, arXiv preprint, https://doi.org/10.48550/arXiv.2406.01465, 2406.01465.

Levin, E., 2026: Tropical cyclone tracks and environmental fields from a 1,000-member deep-learning climate emulator ensemble. Zenodo, URL https://doi.org/10.5281/zenodo.19456834, https://doi.org/10.5281/zenodo.19456834.

Levin, E. L., M.-T. Chien, E. Barnes, H. He, G. A. Vecchi, and W. Yang, 2026a: On the seasonal predictability of the 2020 North Atlantic tropical cyclone season. https://doi.org/10.31223/X5CN1R.

Levin, E. L., G. A. Vecchi, and W. Yang, 2026b: Influence of sea surface temperature patterns and mean warming on past and future Atlantic tropical cyclone activity. *Journal of Climate*, **39 (10)**, 3735–3758, https://doi.org/10.1175/JCLI-D-25-0635.1.

Li, X., J. Ghosh, and G. Villarini, 2023: Bayesian Negative Binomial regression model with unobserved covariates for predicting the frequency of north atlantic tropical storms. *Journal of Applied Statistics*, **50 (9)**, 2014–2035, https://doi.org/10.1080/02664763.2022.2063266.

Moorthi, S., and M. J. Suarez, 1992: Relaxed Arakawa–Schubert: A parameterization of moist convection for general circulation models. *Monthly Weather Review*, **120 (6)**, 978–1002, https://doi.org/10.1175/1520-0493(1992)120⟨0978:RASAPO⟩2.0.CO;2.

Murakami, H., T. L. Delworth, N. C. Johnson, F. Lu, C. E. McHugh, and L. Jia, 2025: Seasonal forecasts of tropical cyclones using GFDL SPEAR and HiFLOR-s. *Journal of Climate*, **38 (9)**, 3601–3620, https://doi.org/10.1175/JCLI-D-24-0356.1.

Murakami, H., G. Villarini, G. A. Vecchi, W. Zhang, and R. Gudgel, 2016a: Statistical–dynamical seasonal forecast of North Atlantic and U.S. landfalling tropical cyclones using the high-resolution GFDL FLOR coupled model. *Monthly Weather Review*, **144 (6)**, 2217–2236, https://doi.org/10.1175/MWR-D-15-0308.1.

Murakami, H., and Coauthors, 2015: Simulation and prediction of category 4 and 5 hurricanes in the high-resolution GFDL HiFLOR coupled climate model. *Journal of Climate*, **28 (23)**, 9058–9079, https://doi.org/10.1175/JCLI-D-15-0216.1.

Murakami, H., and Coauthors, 2016b: Seasonal forecasts of major hurricanes and landfalling tropical cyclones using a high-resolution GFDL coupled climate model. *Journal of Climate*, **29 (22)**, 7977–7994, https://doi.org/10.1175/JCLI-D-16-0233.1.

Raavi, P. H., and K. J. E. Walsh, 2020: Sensitivity of tropical cyclone formation to resolution-dependent and independent tracking schemes in high-resolution climate model simulations. *Earth and Space Science*, **7 (3)**, e2019EA000 906, https://doi.org/10.1029/2019EA000906.

Schneider, D. P., C. Deser, J. Fasullo, and K. E. Trenberth, 2013: Climate data guide spurs discovery and understanding. *Eos, Transactions American Geophysical Union*, **94 (13)**, 121–122, https://doi.org/10.1002/2013EO130001.

Sugi, M., Y. Yamada, K. Yoshida, R. Mizuta, M. Nakano, C. Kodama, and M. Satoh, 2020: Future changes in the global frequency of tropical cyclone seeds. *SOLA*, **16**, 70-74, https://doi.org/10.2151/sola.2020012.

Tang, B., and K. Emanuel, 2010: Midlevel ventilation's constraint on tropical cyclone intensity. *Journal of the Atmospheric Sciences*, **67 (6)**, 1817-1830, https://doi.org/10.1175/2010JAS3318.1.

Tang, B., and K. Emanuel, 2012: A ventilation index for tropical cyclones. *Bulletin of the American Meteorological Society*, **93 (12)**, 1901-1915, https://doi.org/10.1175/BAMSD1100165.1.

Tippett, M., S. Camargo, and A. Sobel, 2011: A poisson regression index for tropical cyclone genesis and the role of large-scale vorticity in genesis. *Journal of Climate*, **24 (9)**, 2335-2357, https://doi.org/10.1175/2010JCLI3811.1.

Ullrich, P. A., and C. M. Zarzycki, 2017: TempestExtremes: a framework for scale-insensitive pointwise feature tracking on unstructured grids. *Geoscientific Model Development*, **10 (3)**, 1069–1090, https://doi.org/10.5194/gmd-10-1069-2017.

Vecchi, G. A., and G. Villarini, 2014: Next season's hurricanes. **343 (6171)**, 618–619, https://doi.org/10.1126/science.1247759.

Vecchi, G. A., M. Zhao, H. Wang, G. Villarini, A. Rosati, A. Kumar, I. M. Held, and R. Gudgel, 2011: Statistical–dynamical predictions of seasonal North Atlantic hurricane activity. *Monthly Weather Review*, **139 (4)**, 1071–1087, https://doi.org/10.1175/2010MWR3499.1.

Vecchi, G. A., and Coauthors, 2014: On the seasonal forecasting of regional tropical cyclone activity. *Journal of Climate*, **27 (21)**, 8065–8087, https://doi.org/10.1175/JCLI-D-14-00158.1.

Vecchi, G. A., and Coauthors, 2019: Tropical cyclone sensitivities to CO2 doubling: roles of atmospheric resolution, synoptic variability and background climate changes. *Climate Dynamics*, **53 (9)**, 5999–6033, https://doi.org/10.1007/s00382-019-04913-y.

Villarini, G., B. Luitel, G. A. Vecchi, and J. Ghosh, 2019: Multi-model ensemble forecasting of North Atlantic tropical cyclone activity. *Climate Dynamics*, **53**, 7461–7477, https://doi.org/10.1007/s00382-016-3369-z.

Villarini, G., G. A. Vecchi, T. R. Knutson, and J. A. Smith, 2011: Is the recorded increase in short-duration North Atlantic tropical storms spurious? *Journal of Geophysical Research: Atmospheres*, **116**, D10 112, https://doi.org/10.1029/2010JD015493.

Villarini, G., G. A. Vecchi, and J. A. Smith, 2010: Modeling the dependence of tropical storm counts in the North Atlantic basin on climate indices. *Monthly Weather Review*, **138 (7)**, 2681–2705, https://doi.org/10.1175/2010MWR3315.1.

Villarini, G., G. A. Vecchi, and J. A. Smith, 2012: U.S. landfalling and North Atlantic hurricanes: Statistical modeling of their frequencies and ratios. *Monthly Weather Review*, **140 (1)**, 44–65, https://doi.org/10.1175/MWR-D-11-00063.1.

Walsh, K. J. E., M. Fiorino, C. W. Landsea, and K. L. McInnes, 2007: Objectively determined resolution-dependent threshold criteria for the detection of tropical cyclones in climate models and reanalyses. https://doi.org/10.1175/JCLI4074.1.

Watt-Meyer, O., and Coauthors, 2025: ACE2: Accurately learning subseasonal to decadal atmospheric variability and forced responses. *npj Climate and Atmospheric Science*, **8 (1)**, 205, https://doi.org/10.1038/s41612-025-01090-0.

Yang, W., T.-L. Hsieh, and G. A. Vecchi, 2021: Hurricane annual cycle controlled by both seeds and genesis probability. *Proceedings of the National Academy of Sciences*, **118 (41)**, e2108397 118, https://doi.org/10.1073/pnas.2108397118.

Young, R., and S. Hsiang, 2024: Mortality caused by tropical cyclones in the United States. **635 (8037)**, 121–128, https://doi.org/10.1038/s41586-024-07945-5.

Zhang, G., M. Rao, J. Yuval, and M. Zhao, 2025: Advancing seasonal prediction of tropical cyclone activity with a hybrid AI–physics climate model. *Environmental Research Letters*, **20 (9)**, 094 031, https://doi.org/10.1088/1748-9326/adf864.

Zhao, M., I. M. Held, S.-J. Lin, and G. A. Vecchi, 2009: Simulations of global hurricane climatology, interannual variability, and response to global warming using a 50-km resolution gcm. *Journal of Climate*, **22 (24)**, 6653–6678, https://doi.org/10.1175/2009JCLI3049.1.

Zhao, M., I. M. Held, and G. A. Vecchi, 2010: Retrospective forecasts of the hurricane season using a global atmospheric model assuming persistence of SST anomalies. *Monthly Weather Review*, **138 (10)**, 3658–3675, https://doi.org/10.1175/2010MWR3366.1.